

Air quality and climate responses to anthropogenic black carbon emission changes from East Asia, North America and Europe



Makliyar Sadiq ^{a, b, 1}, Wei Tao ^{a, 1}, Junfeng Liu ^{a, *}, Shu Tao ^a

^a Laboratory for Earth Surface Processes, College of Urban and Environmental Sciences, Peking University, Beijing, China

^b The Graduate Division of Earth and Atmospheric Sciences, Chinese University of Hong Kong, Hong Kong, China

HIGHLIGHTS

- We model the short-term climatic effects of regional black carbon (BC) emissions.
- Emissions would linearly impact the BC burden over source and nearby downwind areas.
- Some climatic factors preserve a robust linear relationship only in source areas.
- The perturbation of atmospheric circulation complicates much of BC climatic forcing.

ARTICLE INFO

Article history:

Received 17 April 2015

Received in revised form

30 June 2015

Accepted 2 July 2015

Available online 26 July 2015

Keywords:

Black carbon

East Asia

Europe

North America

Climate response

Radiation budget

ABSTRACT

East Asia, North America and Europe are the world largest emitters of anthropogenic black carbon (BC). In this study, the role of each region's anthropogenic BC emissions on domestic air quality and climate is investigated. A ten-year six-member parallel simulation (i.e., with anthropogenic emissions in each region reduced by 0%, 50% or 100%, or increased by 200%, 500% or 1000%) is conducted based on the state-of-the-art Community Earth System Model (CESM). Linearity of the emission-response relationship is examined for a variety of air quality and climate indicators. Generally, a change in BC emissions tend to linearly influence BC concentrations over both source and nearby downwind regions even taking into account the effect of BC-induced climate perturbations. Aerosol optical depth (AOD) and the net radiative flux perturbation at top of atmosphere (TOA) tend to preserve a similar linear relationship to local BC emission changes, with a robust signal confined only to the source areas. However, the response of temperature in most places is inconsistent to BC emission changes. Though the presence of BC in the atmosphere absorbs solar and terrestrial radiation which has a tendency to warm the atmosphere, the perturbed atmospheric circulation induces substantial meridional exchanges of warm and cold air masses, which overpasses the warming tendency of BC exerted on the atmosphere. This indicates that reducing/increasing regional BC emissions immediately ameliorate/deteriorate local air quality proportionally, but the associated effects on climate perturbation may lack a clear trend within the initial 10-year time span.

© 2015 Elsevier Ltd. All rights reserved.

1. Introduction

Black carbon (BC) aerosol, emitted from a variety of combustion processes, affects the Earth's climate system directly through absorbing and scattering the solar radiation, and indirectly through altering the cloud processes as well as the melting of snow and ice

due to its unique physical properties (Bond et al., 2013). Though the freshly emitted BC (hydrophobic BC) is insoluble in water or common organic solvents, its aging processes in which water-soluble substances (e.g., sulfuric acid) accumulate on its surface would enhance its cloud condensation nuclei (CCN) activity. Aging (Onischuk et al., 2003; Oshima et al., 2009) complicates much of the issues of the lifetime and removal rate of BC.

The direct radiative forcing (DRF) is the most commonly studied climate forcing terms for BC (Chung and Seinfeld, 2005; Hansen et al., 2005; Sokolov, 2006), and the BC DRF from all present-day sources was estimated to be $+0.88 \text{ W m}^{-2}$ with 90% uncertainty

* Corresponding author.

E-mail address: jfliu@pku.edu.cn (J. Liu).

¹ M. S. and W. T. contributed equally to this work.

bounds of +0.17 to +1.48 W m⁻². In addition, it was found that BC contributed to the warming of Arctic regions (Sand et al., 2013; Shindell and Faluvegi, 2009). The semi-direct effect refers to the alteration of cloud distribution by DRF of BC. The RF of BC induces adjustments of different time scales within the climate system. Chung et al. (2002) found that radiation absorbing aerosol (e.g. BC) could warm the atmosphere while cool the land surface below, stabilize the boundary layer, reduce the evaporation and sensible heat flux from the land, and furthermore impact the monsoon dynamics in South Asia. Menon et al. (2002) and Ramanathan et al. (2005) found that regional climate trends of temperature fields and hydrological cycle could be attributed to lifting BC atmospheric burdens in Asia. The large uncertainty in modeled BC RF could be attributed to the diversity in estimating BC's atmospheric burden (e.g., emission, lifetime) and optical properties (e.g. mass absorption cross section and forcing efficiency) (Bond et al., 2013). Besides, the radiative forcing of BC depends highly on the altitude location (Ban-Weiss et al., 2012), vertical profile (Samset et al., 2013), and mixing state with co-emitted species (Cappa et al., 2012; Chung and Seinfeld, 2002; Haywood and Shine, 1995).

The cloud and ice/snow effects of BC even remain more uncertain (Denman et al., 2007; Flanner et al., 2007; Heintzenberg and Charlson, 2009). Nonetheless, the total climate forcing integrating all forcing terms was estimated to be +1.1 W m⁻² with 90% uncertainty bounds of +0.17 to +2.1 W m⁻². BC is potentially the second most important climate warming agent only inferior to carbon dioxide (Bond et al., 2013), whose RF was estimated to be 1.66 W m⁻² (Forster et al., 2007). The predominant sources for BC include fossil fuels (38%), solid fuels (20%) and open burning (42%), and are largely contributed by anthropogenic combustion (Bond et al., 2004). This motivates the establishment of sound emission metrics for BC in mitigation of its adverse climate impacts. However, to our knowledge, little literature has investigated how BC emission in a certain region changes along the gradient (i.e., BC emissions are changed by -100%, -50%, 0%, 200% and 1000%, respectively) would impact the global climate.

In this study, we utilized a fully-coupled earth system model CESM to evaluate the global short-term climate response due to anthropogenic BC emitted from East Asia, North America and Europe, which are considered to be the biggest contributors in global anthropogenic BC emissions. Rather than identifying the equilibrium climate response from a BC emission perturbation (which may take more than century's period of simulation), this study focuses on the "closest to real" short-term effect (Jacobson, 2010) of BC on our environment. Specifically, we'd like to understand whether the disturbance of air quality and regional climate in different areas response linearly or nonlinearly to the fluctuation of BC emissions in a particular region. Only direct and semi-direct effects of BC on radiation are involved in this configuration. Therefore, the result reflects a short-term climate perturbation in a particular configuration of CESM. From there, we evaluate the extent that a robust emission-response relationship (i.e., air quality and climate perturbations) exists for BC from different regions. This may acknowledge policymakers the potential outcomes if BC emissions over the region are well controlled or uncontrolled.

The configuration of CESM is adapted in this study to allow chemistry processes coupled into general circulation model. That atmospheric component of CESM (i.e., CAM-Chem) utilized in this experiment has a comprehensive treatment of aerosol processes and its interaction with climate. We investigate various indicators related to climate perturbation, including black carbon burden, aerosol optical depth, radiation budget, cloud cover, the surface air temperature (SAT), surface pressure and wind fields, etc. We describe our experiment design and model configuration in Section 2, and show the air quality relevant results in Section 3 and climate

relevant findings in Section 4. Finally, conclusions are drawn in Section 5.

2. Methods

2.1. Model description

The Community Earth System Model (CESM) version 1.1.2 (released in July 2013) was used in this study. CESM is a fully coupled climate model with components of an atmospheric model of Community Atmospheric Model Version 4 (CAM4), a land model of Community Land Model Version 4 (CLM4), an ocean model Parallel Ocean Program Version 2 (POP2), models of sea ice, land ice and river, and a high-performance coupler. The 1.1z release of CESM has been scientifically validated, and the outputs of multi-decadal model runs have been evaluated (<http://www2.cesm.ucar.edu/models/scientifically-supported>). CAM-Chem (CAM4 with implementation of chemistry) has its chemistry process expanded but mostly equivalent to MOZART-4 (Lamarque et al., 2012). Though, interactions between climate and chemistry processes are only through radiation, CAM4 does not include cloud–aerosol interactions (i.e., aerosols indirect effect). CAM4 was released as part of CESM and proved scientifically valid through simulations and comparisons with observation data (Collins et al., 2004; Neale et al., 2010). The finite volume dynamic core is the default in CAM4 due to its superior tracer transport properties. Deep convection is parameterized using the Zhang and McFarlane (1995) scheme. Other parameterization methods on clouds and precipitation processes can be found in Boville et al. (2006). Processes in the planetary boundary layer are parameterized following Holtlag and Boville (1993).

Dry deposition in CAM-Chem is calculated following the resistance approach (Wesely, 1989). The computation of canopy resistance in CAM-Chem takes advantage of its coupling to Community Land Model. The BULK scheme in CAM-Chem uses fixed dry deposition velocities of black and organic aerosols as 0.1 cm s⁻¹ over all surfaces (Lamarque et al., 2012). Wet removal of soluble gas-phase species is the combination of two processes: in-cloud, or nucleation scavenging (rain-out) and below-cloud, or impaction scavenging (washout). Removal can be seen as a simple first-order loss process.

There are three aerosol treatment methods in this model, BAM (Bulk Aerosol Model), MAM3 (3 Mode Aerosol Model) and MAM7 (7 Mode Aerosol Model). In this study, the aerosol treatment scheme we utilized is based on the Bulk Aerosol Model (BAM) and assumes the lognormal distribution of black carbon aerosols follows a mean radius of 11.8 nm, geometric standard deviation of 2.00 and density of 1.0 g cm⁻³. We didn't use MAM (both MAM3 and MAM7 include various indirect effects of aerosols) since this paper mainly focuses on the direct and semi-direct effects of black carbon on the climate, which relies less on aerosol size distributions and thus is associated less to the uncertainties in modeling the indirect effects. Black carbon in the BULK aerosol scheme is simulated as two separate tracers: one is hydrophobic (CB1) which represents black carbon particles have insufficient coating of soluble materials and thus cannot be treated as cloud condensation nuclei (CCN), and the other is hydrophilic (CB2) which represents internally mixed BC which can activate cloud droplets. The conversion of carbonaceous aerosols from hydrophobic to hydrophilic is assumed to occur as a fixed aging timescale of 1.6 days (Tie et al., 2001).

2.2. Model configuration

The model is set up with a grid resolution of 1.9 × 2.5°

horizontally and 26 layers vertically up to about 4 hPa. A set of simulations, targeting on the effects of regional BC emissions on the climate, is set for three regions: East Asia (EA), North America (NA) and Europe (EU). Regions are defined roughly along the border shown in Fig. 1. The simulation period (starting from 2000) is set for 10 years since our aim is mainly to investigate the short-term climate response. Ocean model (POP2), along with other components of CESM remains active. Emission data are from CESM's data repository: <https://svn-ccsm-inputdata.cgd.ucar.edu/trunk/inputdata/>. Emission rate of BC is based on inventory of Bond et al. (2004). The anthropogenic emissions of black carbon are determined for 1996. Table 1 summarizes total black carbon emissions for individual regions. Over these three targeted regions, anthropogenic emissions are dominated by EA and biomass burning emissions are trivial in any of the three regions.

To evaluate the effect of regional BC emission on global climate, we conducted a set of sensitivity tests in which black carbon emissions from each region is either increased or decreased. Specifically, for each region its BC anthropogenic emissions are multiplied by factors of 0, 0.5, 1, 2, 5, and 10, separately, while emissions outside the region remain unchanged. Multiplication is done both to hydrophilic and hydrophobic black carbon emissions, for both of them having significant climate effects on our earth system. Biomass burning source of black carbon is not modified in this study, since natural sources of BC is much difficult to control compared to the anthropogenic emissions.

Similar to the base, the simulations are run for 10 years starting from the year 2000. The results of 10 years simulations are compared to the base simulation. Linear correlation analysis is conducted between the targeted variables (e.g., BC concentrations, AOD, short-wave and long-wave radiation fluxes at the top of the atmosphere (TOA), etc.) and emission changes. Coefficient of determination (i.e. R^2) is used to illustrate the regions where air quality or climate perturbations vary consistently to emission changes.

3. Chemical response to regional emission changes

3.1. BC concentrations

The simulated 10 years annual mean surface BC concentrations

Table 1
Budget of Black Carbon emissions from East Asia, North America and Europe.

Regions	Emission (Tg yr ⁻¹)		
	Anthropogenic	Biomass burning	Total
EA	1.62	0.03	1.65
NA	0.50	0.12	0.62
EU	0.57	0.04	0.61

are shown in Fig. 2. These results are calculated by subtracting the base simulation of each perturbation runs from sensitivity runs. The difference indicates the contribution of BC emissions from individual regions to the global BC burden. Thus, black carbon has its largest loading near the source region. Since BC has a relatively short lifetime of several days (Forster et al., 2007), the reach of regional influence is mainly confined to the downwind regions near the source. For example, turning off BC emissions from EA will lead to about 1–10 $\mu\text{g kg}^{-1}$ decrease in surface BC concentrations over eastern China, 0.01–0.1 $\mu\text{g kg}^{-1}$ decrease over western Pacific and less than 0.01 $\mu\text{g kg}^{-1}$ over the western U.S. Similarly, turning off anthropogenic BC emissions from NA will lead to 0.1–1 $\mu\text{g kg}^{-1}$ reduction in domestic BC concentrations, and about 0.001–0.01 $\mu\text{g kg}^{-1}$ reduction over West Europe and North Africa. Turning off EU emissions will significantly decrease the surface BC concentrations over the Eurasian continent as well as North Africa, but may enhance the surface BC level by up to 1 $\mu\text{g kg}^{-1}$ over northeastern China. This is probably caused by the EU BC induced circulation changes which decrease air pollution ventilation over EA. For other secondary pollutants (e.g., ozone, sulfate and secondary organic aerosols), however, the change in BC emissions generally has little impact on their concentrations (see Figs. S1–S3 in the supplementary materials).

When doubling anthropogenic BC emissions in a region, in most cases the surface BC burdens tend to increase, except a few places over southern hemisphere. Comparing to the 100% BC reduction cases (plots in first row of Fig. 2), the pattern in BC burden change resulting from doubling BC emissions is close to those with BC emissions removed, but with a reversed sign. However, for NA and EU emissions, a factor of 2 change in BC emissions (either increase or decrease) will generally enhance the surface BC burdens over northeastern China including Beijing. This indicates that BC

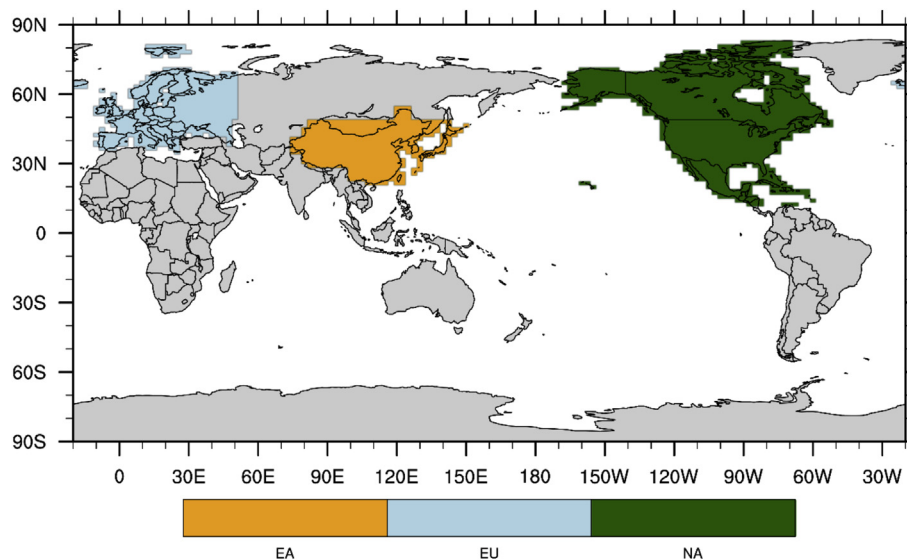


Fig. 1. Schematic map of regional mask of East Asia(EA), Europe(EU) and North America(NA).

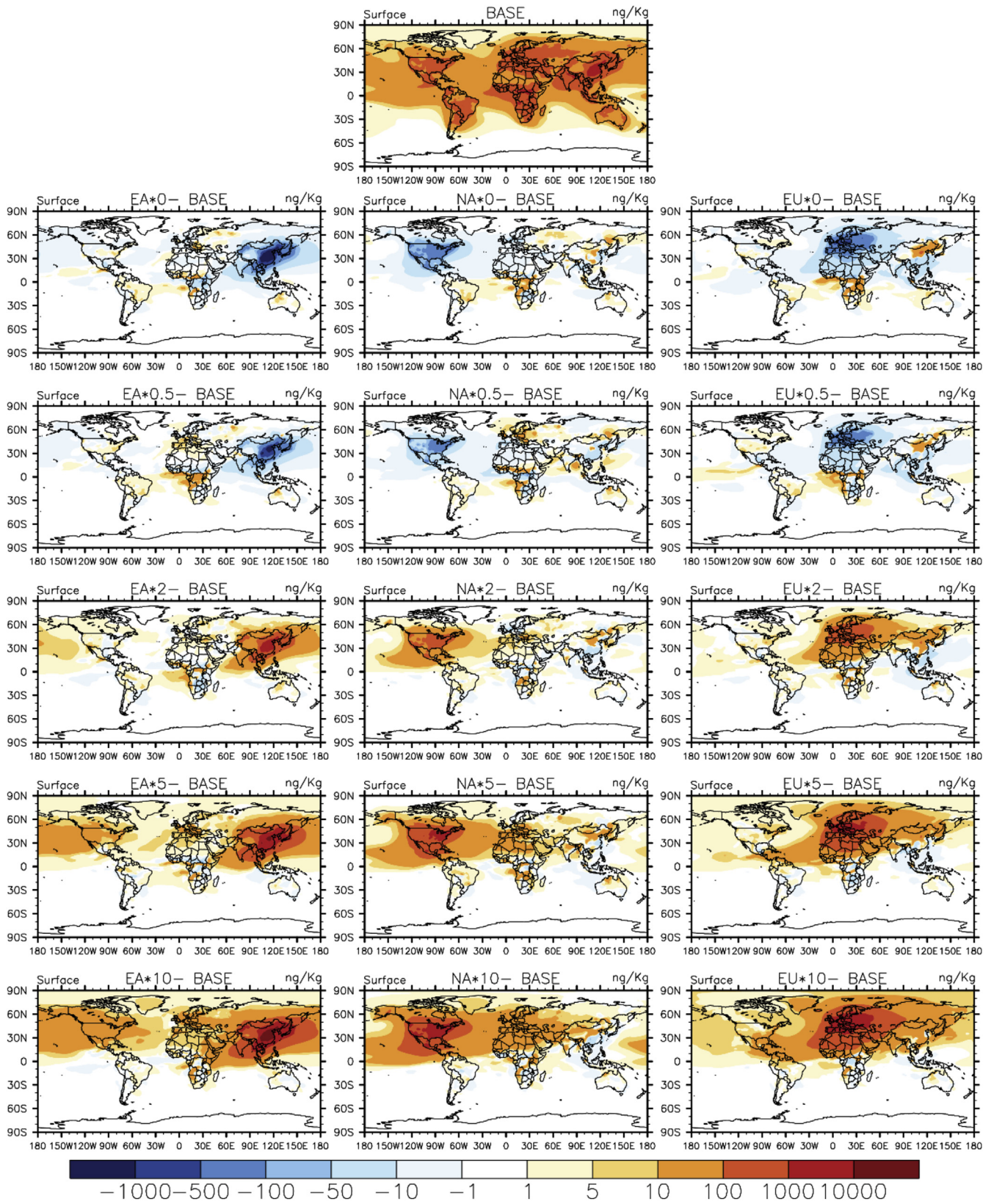


Fig. 2. Surface BC concentrations in BASE run and changes in surface BC concentrations (unit: ng/kg) caused by a decrease (by -100%, and -50%) or an increase (by a factor of 2, 5, and 10) of BC emissions from EA (left), NA (middle) and EU (right).

induced climate perturbation at a hemispheric scale may dominate the BC burden changes.

In order to understand the linearity between regional emission perturbations and global concentration changes, we calculate the linear regression and show the distribution of associated coefficient of determination (i.e., the R^2) at each surface grid in Fig. 3. For BC emitted from each region, responses of BC concentration to emission perturbation are close to linear ($R^2 > 0.95$) over the source and downwind regions, but become nonlinear when approaching major BC source regions or the southern hemisphere. This linear relationship preserves at higher altitudes (not shown) or with the 1000% emission scenario excluded (see Figs. S4 and S5 in the supplementary materials), indicating a robust linear source-receptor relationship over the source region even with the adjustment of BC induced local climate changes (hereafter, local indicates the source region of BC). This is consistent to the findings in Liu et al.

(2009), who found the transport of BC is linear in the chemical transport model MOZART-2.

3.2. Aerosol optical depth (AOD)

AOD measures the integrated optical thickness of all types of aerosols in an atmospheric column. Aerosols' column number density, mixing state and light extinction efficiency determine the magnitude of AOD (Liu et al., 2013). Therefore, when BC loading changes, AOD will follow, but this change may not only represent the BC burden changes. As shown in Fig. 4, AOD over the eastern China varies consistently with BC emission changes. However, any perturbations in EA BC emissions will lead to an enhancement of AOD over the Mongolia. Beside the EA source region, a dipole variation pattern of AOD emerges over north and tropical Africa. This indicates that BC induced climate change (e.g., circulation

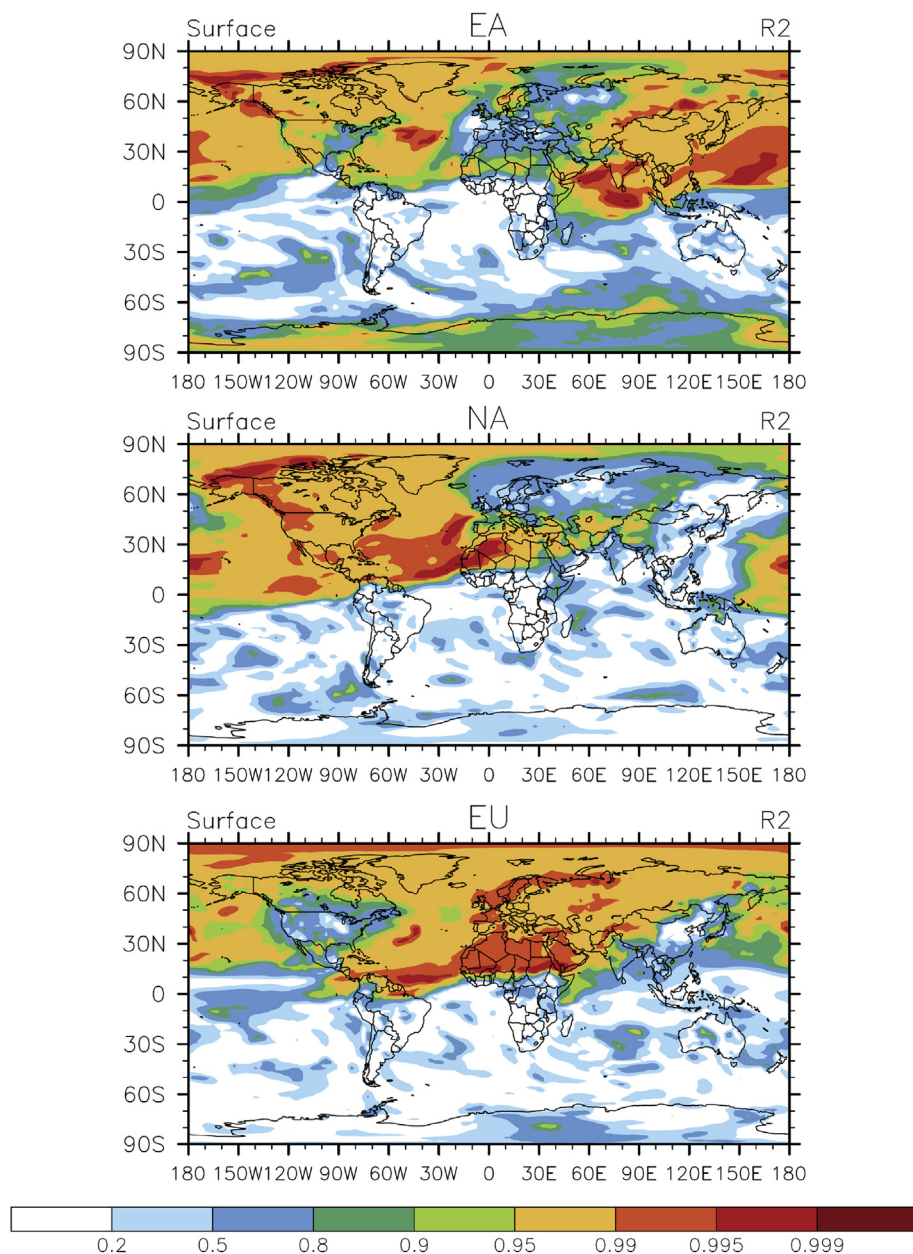


Fig. 3. Distribution of coefficient of determination (R^2) between regional anthropogenic emissions perturbations (i.e., 0%, 50%, 100%, 200%, 500% and 1000% of the base case) over EA (top), NA (middle) and EU (bottom) and the corresponding BC concentration changes in the surface layer.

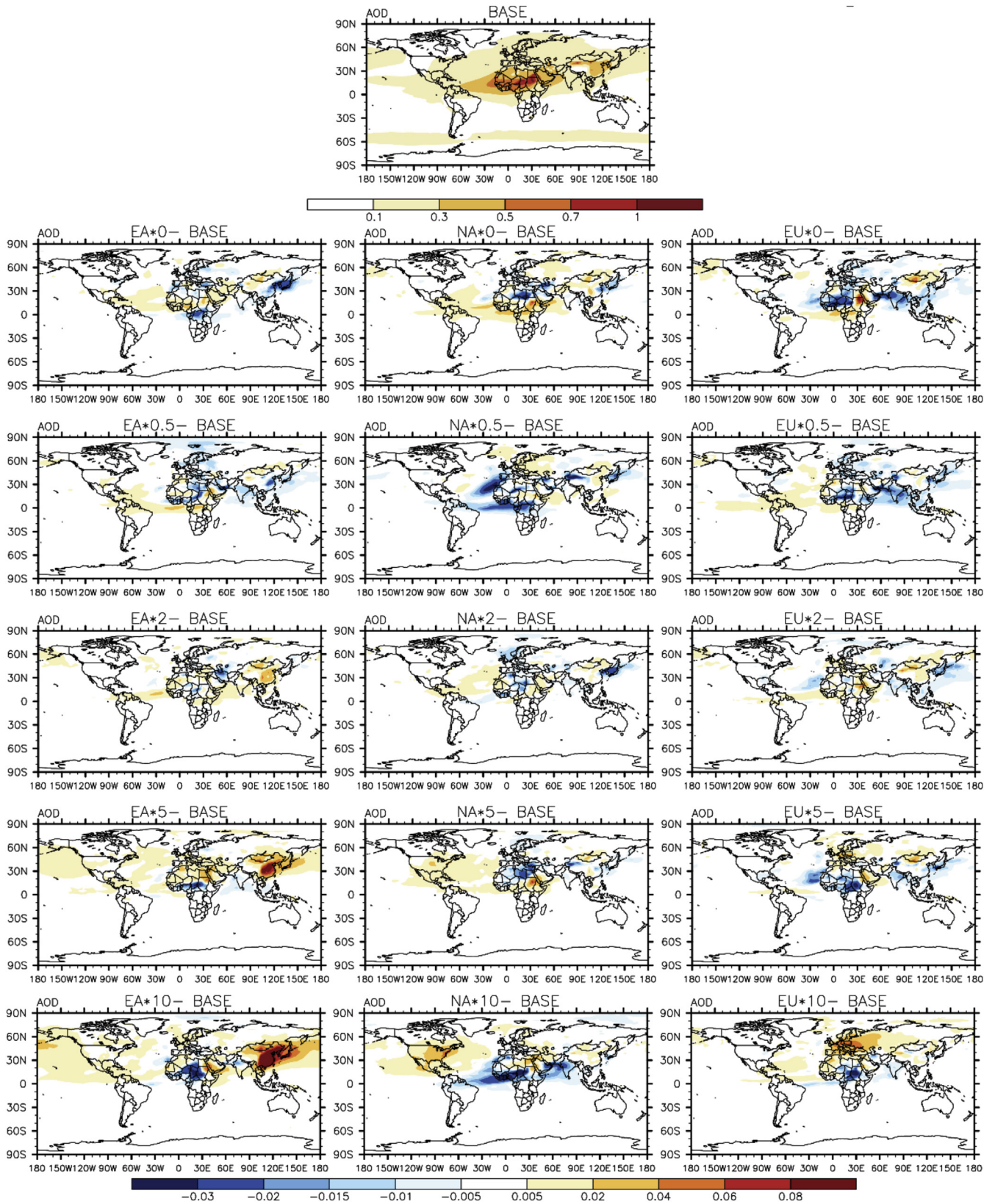


Fig. 4. Same as Fig. 2, but for AOD.

pattern and precipitation) may dominate the influence of concentration changes and the associated climate forcing of all aerosol species beyond the source region.

A factor of 2 change in NA BC emissions has little effect on domestic AOD, but has a larger impact over north and central Africa. The variations of global AOD do not consistently follow the

emission changes in NA, except over the source region. Similarly, a reduction of BC emissions in EU is associated with a stronger AOD perturbation over the north and central Africa than an emission increase in EU. In addition, any perturbation of BC emissions from EU may result in a reduction of AOD over the north Indian Ocean and the Indian subcontinent.

Fig. 5 shows the distribution of coefficient of determination between emission perturbations and AOD changes. Near the source, changes in AOD generally follow a linear relationship to BC emission changes ($R^2 > 0.9$). As for EA emissions, besides eastern China and western Pacific, a linear relationship ($R^2 > 0.8$) extends eastward and covers almost entire North Pacific. This indicates a robust association between BC emissions from EA and aerosols optical properties over the Pacific Ocean. For BC from NA and EU, however, linear relationship keeps only at the source region, except some leakages over the subtropical eastern Pacific (for NA BC) and

mid-Asia (for EU BC). This indicates that the linkage between BC emissions in NA (or EU) and aerosols optical properties is rather complicated outside of the source region.

Above analysis demonstrates that changes in BC emissions over a region usually proportionally modify domestic AOD, and may have an impact beyond the source region and affect chemical fields besides the BC particle. The climate change induced evolution of other aerosol species (e.g., dust and biomass burning aerosols) sometimes may drive an even larger forcing to balance or reinforce the direct forcing from BC perturbations. In addition, although the source-receptor relationship of BC evolution is found to be linear in many places in Section 3.1, the forcing of BC on other aerosols distribution features nonlinear and regional dependent. This complicates the processes in aerosol–aerosol, aerosol–radiation as well as aerosol–climate interactions.

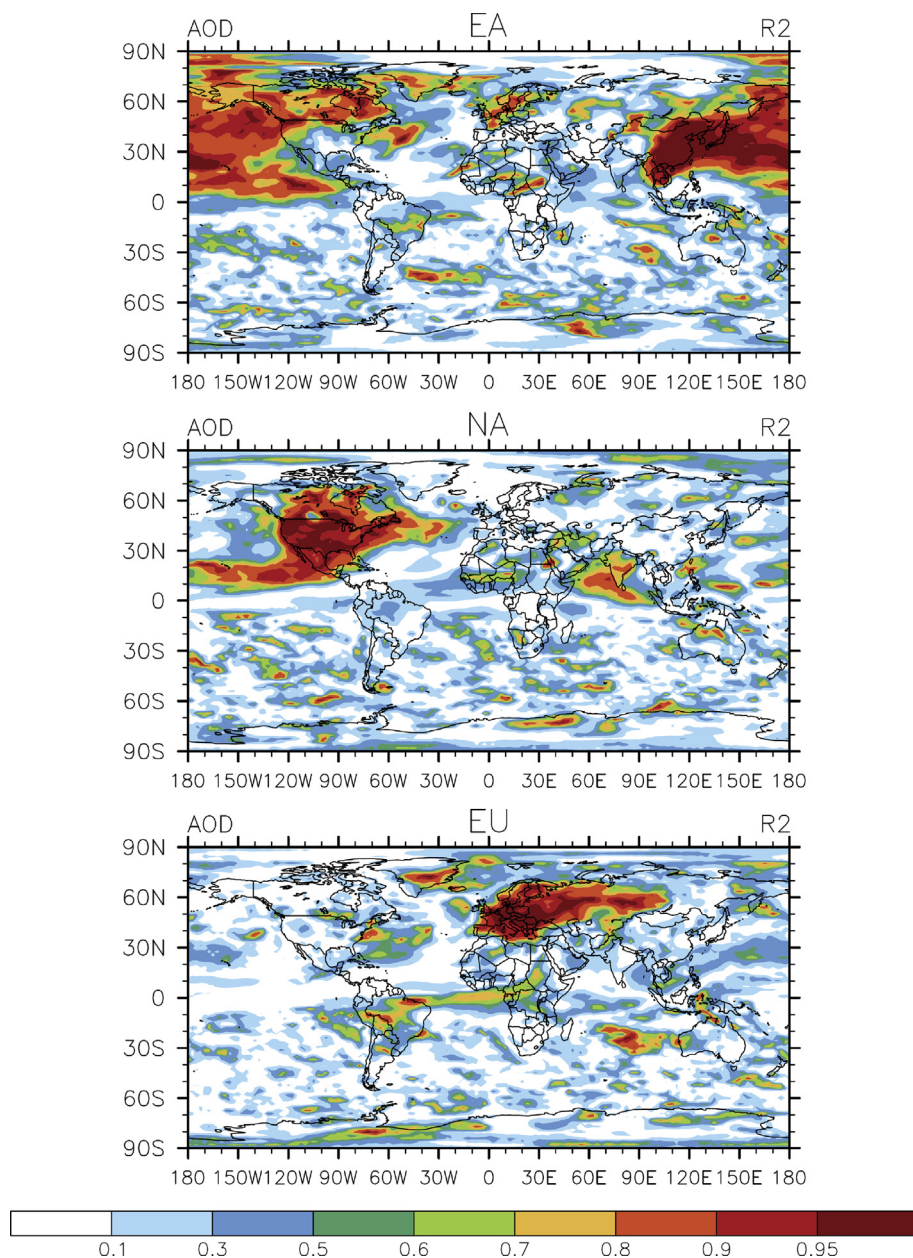


Fig. 5. Same as Fig. 3, but for AOD.

4. Climate perturbation due to regional BC emission changes

4.1. Radiative flux perturbation at top of the atmosphere

The net flux of incoming solar radiation and outgoing terrestrial radiation at top of the atmosphere (TOA) determines the global budget and associated energy balance of the earth system. Clouds and absorbing aerosols (e.g., BC) strongly influence both the shortwave and longwave transmissions. Therefore, any changes in BC burden even at the regional scale may disturb the radiation at TOA, consequently the earth energy balance. Fig. 6 shows the radiative flux perturbation (RFP, shortwave plus longwave) at TOA regarding the change of BC emissions from each continental region.

Since temperature over all land and sea surfaces is unfixed, the radiative perturbation shown here is different to the radiative forcing in which troposphere or surface (e.g., sea) temperature is fixed (Forster et al., 2007; Hansen et al., 2005; Shine et al., 2003) or the instantaneous radiative forcing estimated by a radiation alone model (Hansen et al., 1997). Results in this study represent the potential climate response to the change of a climate forcer at the initial stage, in which the earth system is far from equilibrium. It would show policymakers the possible climate and air quality response if a climate forcer is removed or reinforced.

As shown in Fig. 6, responses of RFP to BC emissions depend strongly on location as well as the magnitude of emission. Over EA, a reduction of local BC emissions is generally associated with a

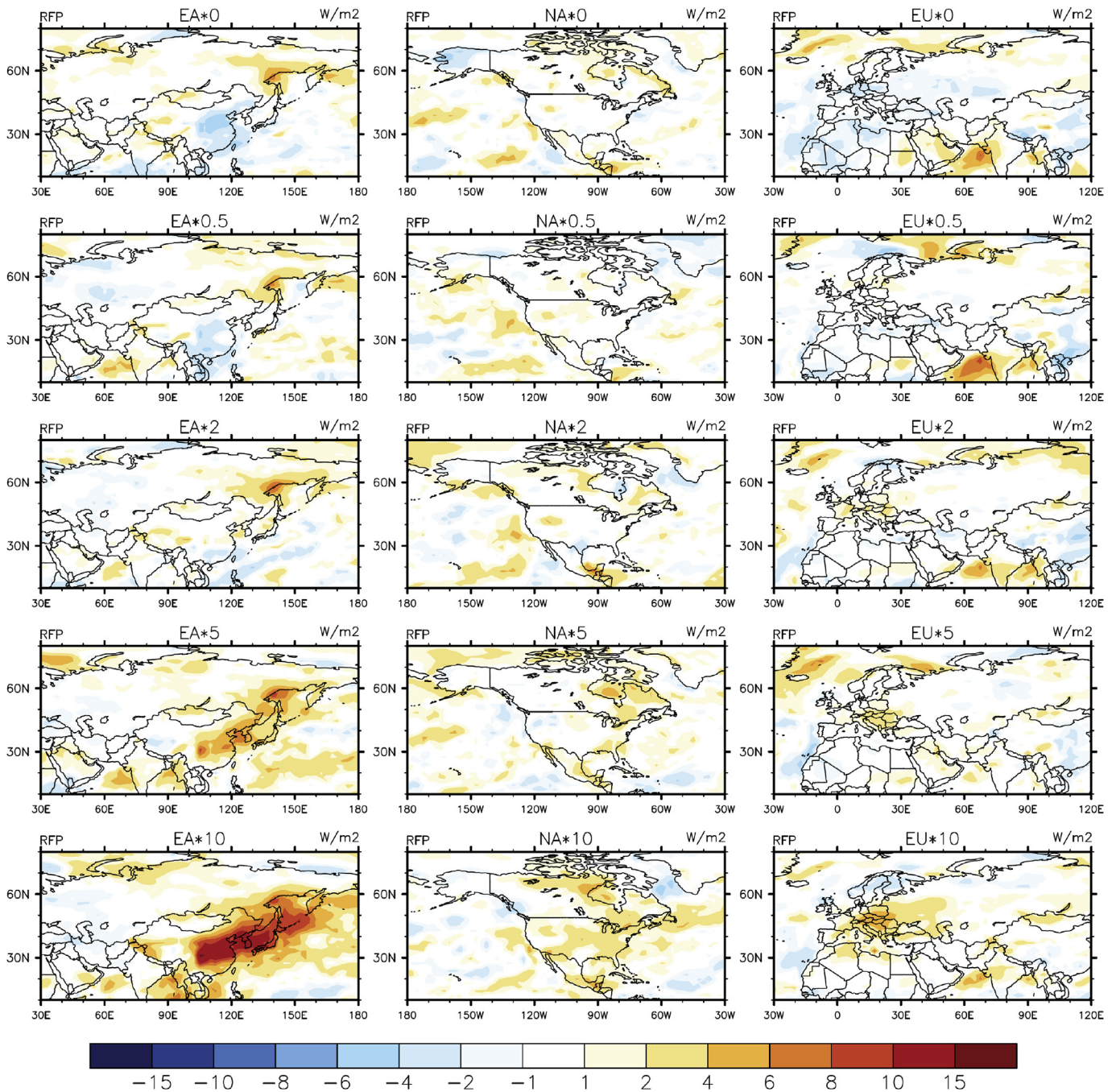


Fig. 6. Same as Fig. 2, but for the changes of net radiative flux perturbations at TOA over EA (left), NA (middle) and EU (right).

decrease in net radiation flux at TOA. This is mainly because fewer BC absorbs less solar and terrestrial radiation and thereby traps less energy in the atmosphere. A similar weaker RFP response to local BC reduction is found over EU, but is unable to observe over NA. When BC emissions increase, the RFP response becomes positive, particularly for EA emissions. The response of RFP is similar to AOD perturbations as found in Fig. 4, namely an increase in BC emissions tends to enhance the atmospheric loadings of aerosols and their optical depth. Rather than reflecting solar radiation, this increase of AOD allows more radiation energy being absorbed by the atmosphere and therefore has a warming tendency. Over EA, a factor of 2 increase in local BC emissions leads to a weak positive RFP over northern China and a weak negative RFP over southern China. However, a factor of 5 or 10 increase in BC emissions from EA tends to trigger a large positive RFP (up to 15 W m^{-2}) over eastern China and $4\text{--}10 \text{ W m}^{-2}$ along the east coast of Eurasian continent. Similar trend is found for EU, where up to 5 W m^{-2} RFP is found over Austria when BC emissions from EU are increased by a factor of 10. Over NA, a factor of 5 or 10 increase in BC emissions will significantly enhance the RFP over the eastern NA, but the signal is much weaker than that of either EA or EU.

Besides domestic response, the RFP change may extend to the nearby region. For instance, either increase or decrease in BC emissions from EA may enlarge RFP over the Eastern Russia. This is mainly determined by the decrease of cloud amount over the region whether EA BC emission increases or decreases (Fig. S6). Similarly, BC emission change (particularly a decrease) in EU may induce a large positive RFP change ($>5 \text{ W m}^{-2}$) over the north Indian Ocean, which might be linked to the reduction of AOD over the Indian subcontinent (Fig. 2). This extended RFP response results mainly from the change of reflection properties of the atmosphere, which is largely influenced by cloud and aerosol activities. Therefore, the radiative perturbation induced by a regional climate forcer could be propagated to other places via teleconnected chemistry–climate interactions.

Fig. 7 shows the relationship (represented by R^2) between BC emission perturbations and RFP changes at TOA. Linear associations persist mainly above the source and nearby downwind regions. This pattern is very close to AOD, but with a smaller R^2 value in general. Spatially, over EA the RFP change is almost proportional to local BC emission changes over east and northeast China, the Yellow Sea, Sea of Japan and Sea of Okhotsk. However, this linear relationship disappears whenever the outflow of EA pollution reaches western Pacific, where both AOD and BC concentration response linearly to emission changes. Similar results are found over EU and NA. Further decomposing RFP into net shortwave flux perturbation and outgoing longwave flux perturbation reveals that the RFP change at TOA is mainly determined by the shortwave flux changes, which is strongly influenced by the presence of clouds. As shown in Fig. S6, the change of local BC emissions leads to north-south shifting of a belt of cloud residing over the source and downwind oceanic region, which strongly disturb the amount of solar radiation that is being absorbed by the earth surface. We also investigate the clear-sky radiation budget and find that linear association between RFP and local BC emissions generally covers a broader area except NA (which is mainly influenced by the perturbation of longwave radiation. Figures are not shown).

4.2. Regional temperature perturbation

The change in RFP disturbs the energy balance of the climate system. When BC presents in the atmosphere, it absorbs both solar and terrestrial radiations and warms the air nearby, but may partially block solar radiation penetrating to the Earth's surface. As found by (Ban-Weiss et al., 2012), black carbon near the surface

causes surface warming, whereas black carbon near the tropopause and in the stratosphere causes surface cooling. This warming/cooling effect changes the lapse rate of the atmosphere, which further perturbs the dynamics in support of cloud and aerosols distribution. Therefore, the change in temperature is a balanced result from all of these feedbacks.

As mentioned above, this study allows SST change, and focuses on the initial period of a fully coupled climate simulation. Therefore, results presented here do not reflect a stable temperature response since it is impossible for the atmosphere-ocean system to reach equilibrium in such a short period. The climate response may be strongly affected by the internal variability of the climate system. To minimize the potential influence from internal climate variability, global climate simulations either use a number of ensemble runs, each of which assigns a slightly different initial condition, or rely on sets of parallel simulations by different climate models (like the climate models inter-comparison project). In this study, we conduct six parallel runs in which only BC emissions of a specific region are modified. Based on these runs, we examine the consistency between BC burden changes and surface temperature changes. In this manner, we attempt to reduce the influence of internal variability to some degree.

Fig. 8 shows the short-term temperature change at 850 hPa in response to BC emission changes (for comparison purposes, the response of surface temperature is given in the supplementary materials, see Fig. S7). Over EA, turning off BC emissions leads to a cooling effect at 850 hPa mainly near the source region. Conversely, significant increases in BC emissions enhance 850 hPa temperature over the downwind mid-latitude regions (i.e., Mongolia, Northeastern China, Japan and western Pacific). This pattern is consistent to the perturbation of RFP at TOA (Fig. 6) and the maximum temperature change happens over western Pacific near 160°E . Besides this pattern, changes of EA emissions lead to a robust dipole pattern in temperature change over the Arctic region, i.e., a warming tendency over the northwestern Russia and a cooling tendency over the northeastern Russia. The former appears stronger when EA emission changes are less than a factor of 5, but tends to diminish when EA emissions increase by a factor of 10. In addition, when the warming tendency over the North Pacific increases, a cooling tendency over north of Aleutian Islands develops and becomes deeper as more BC emissions are released from EA. Similarly, based on the Community Climate System Model version 3 (CCSM3), Zhang et al. (2011) found that tripling the anthropogenic aerosols (including sulfate, BC, OC, etc.) over China and India would lead to a large warming over the USA and southern Canada in winter and cooling in summer.

Over North America, a reduction of local BC emissions usually results in a cooling zone over the northeastern U.S. and a warming zone over the western U.S. As BC emission increases, the warming effect expands to the entire U.S. (Fig. 8). However, over western Canada, temperature change at lower altitude is complicated. Substantial cooling is observed when NA BC emissions are increased by a factor of 5 or 10. In addition, similar to EA, a weak warming tendency occurs extending to the western North Atlantic. Similar to NA, a change of BC emissions over Europe does not show a consistent change in 850 hPa temperature in most places except the Mediterranean Sea, where an increase/decrease in BC emissions from EU tends to enhance/reduce the 850 hPa temperature there. Over the Arctic, the emission-temperature relationship is rather complicated and behaves nonlinear, indicating that EU BC induced dynamic perturbations overpass its direct warming effect.

Fig. 9 shows the linearity of the response of 850 hPa temperature to BC emission changes from a region. Higher linearity of emissions-temperature relationship occurs at a mid-latitude belt spanning from western China to western Pacific in response to EA

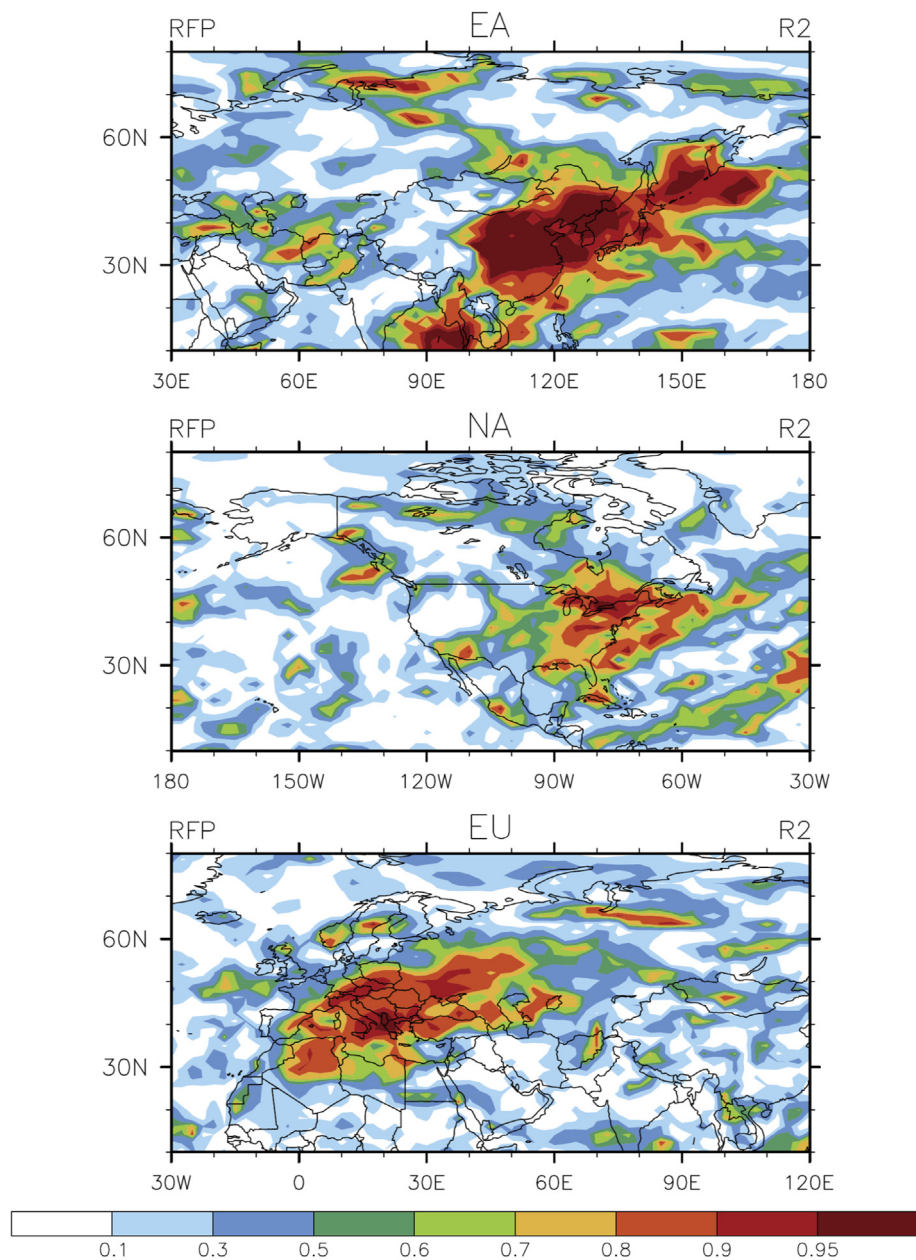


Fig. 7. Same as Fig. 3, but for radiative flux perturbation at TOA.

emission changes, with R^2 values in general larger than 0.8. However, as illustrated in Fig. 10, the associated annual mean temperature variation is less than 0.1 K over the rectangle region (shown in Fig. 9) in response to a factor of 2 change in EA BC emissions (represented by the slope of the regression line). Over NA, changing BC emissions may induce a linear temperature response over the northeastern U.S. and Gulf of Mexico (Fig. 9). The associated sensitivity follows that double BC emissions from NA may enhance the 850 hPa temperature by 0.04 K over the rectangle region near coast of northeastern U.S. This value is a factor of 2 lower than that of EA since BC emissions from NA is roughly half of EA. While for European emissions, consistent temperature response is observed over a broad area covering the Mediterranean Sea and north of Algeria and Libya. However, the slope of the regression line (i.e., Fig. 10) is comparable to that of EA even total BC sources from EA are more than a factor of 2 larger than EU. This indicates that over

the Mediterranean Sea and North Africa, the sensitivity of temperature to BC emission changes could be larger than these places over western Pacific.

4.3. Pressure and wind field changes

Interactions between BC burden and temperature changes are rather complicated. Temperature perturbation is initiated by BC induced change in radiative heating. As temperature increases, the atmosphere has a tendency to disturb the pressure as well as wind fields. The latter drives warm/cold air mass flowing from one place to another, modifies cloud activities, and further disturbs radiation and temperature. Therefore, the temperature change shown in Fig. 8 is a balanced result from both the effect of BC on radiation (i.e., Fig. 6) and the heat transfer along air mass movement.

Fig. 11 shows the surface pressure and wind field changes in

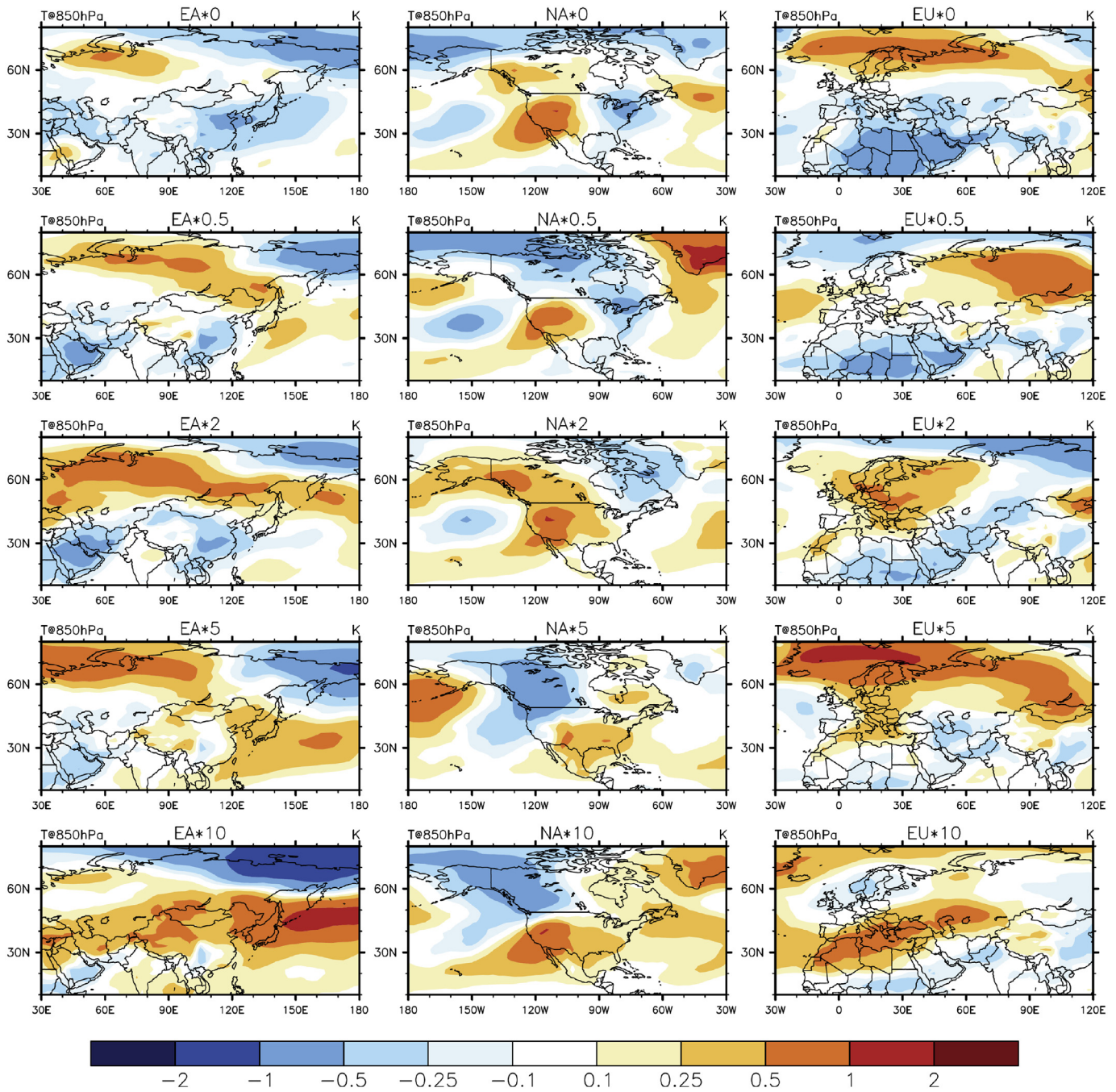


Fig. 8. Same as Fig. 6, but for the temperature changes at 850 hPa.

response to local BC emission changes. In all cases, changes in BC emissions from EA tend to induce positive anti-cyclonic anomalies over the northeastern China and eastern Russia, which generates a tendency to enhance the advection of mid-latitude warm air mass into Mongolia and eastern Russia, and raise the temperature there. In addition, the strong anti-cyclonic anomaly over northeastern China tends to block the intruding cold air from Siberia and intensify the cyclonic anomaly over the northeastern Russia (east of 150°E) and magnify the cooling tendency there. At the same time, it strengthens the intrusion of moist maritime air from western Pacific to southeastern China and enhances the cloud amount and reflection, leading to a cooling effect there.

The change of BC emissions over NA is associated with large

surface pressure and wind fields perturbations. In general, an anti-cyclonic anomaly over the Aleutian Islands in companion with a cyclonic anomaly over northeastern NA appears whenever NA BC emission changes. Specifically, as BC emissions from NA reduce, the surface pressure over northeastern Canada decreases, which generates a tendency to intensify the northwestern wind and lower the temperature at northeastern U.S. As BC emissions increase, an anti-cyclonic anomaly emerges over the northwestern Atlantic. It gradually shifts towards the east coast of NA and has a tendency to weaken the anti-cyclonic anomaly residing over the eastern Canada. The emerge of the anti-cyclonic anomaly near east coast of NA triggers an northward anomaly wind above the east coast of U.S. and warm the temperature over the eastern U.S.

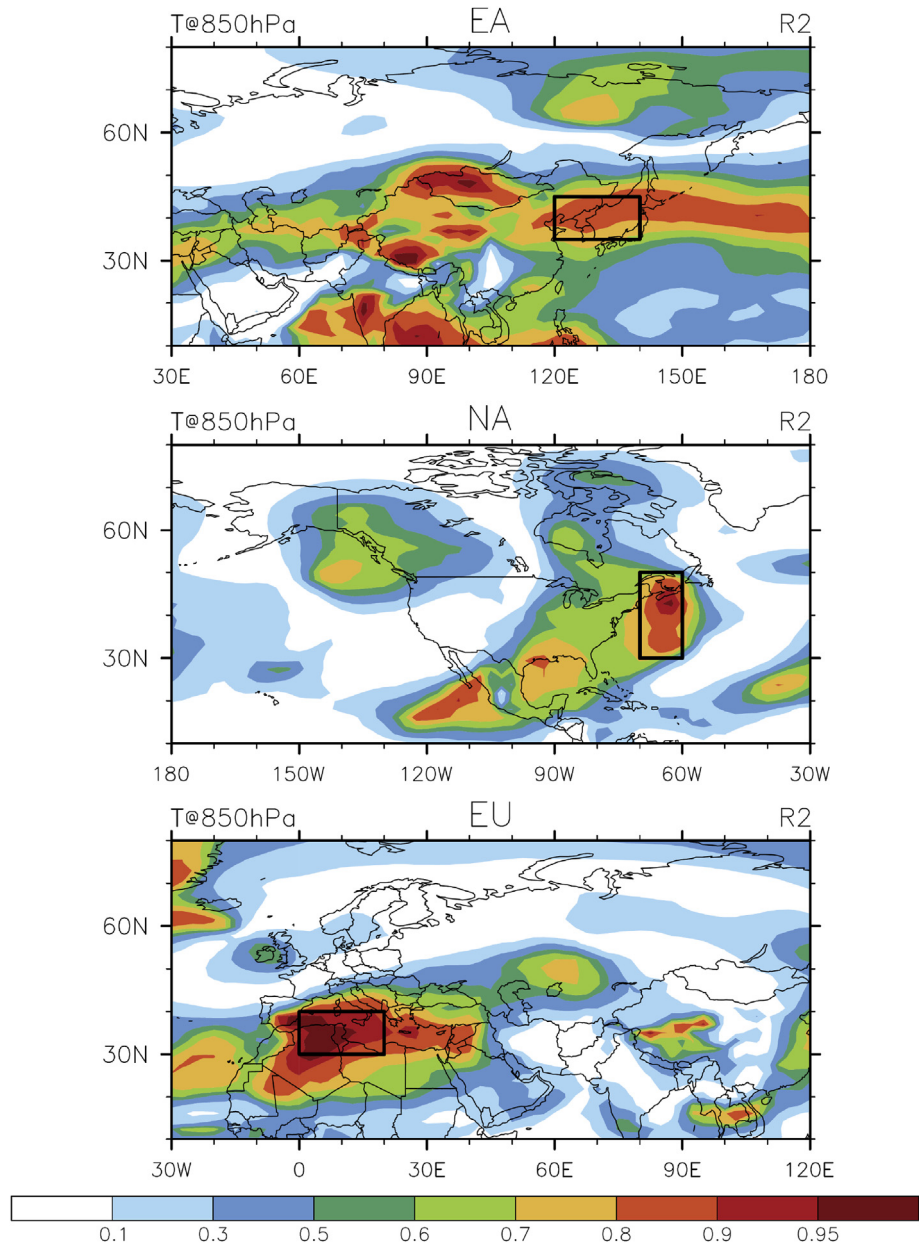


Fig. 9. Same as Fig. 3, but for temperature perturbations at 850 hPa.

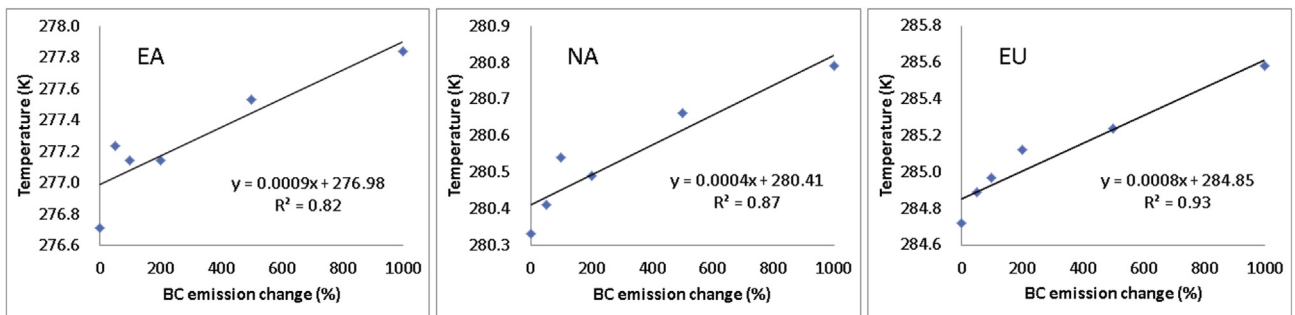


Fig. 10. Sensitivity of annual mean 850 hPa temperature averaged over the rectangle region shown in Fig. 9 to BC emissions changes in East Asia (left), North America (middle) and Europe (right).

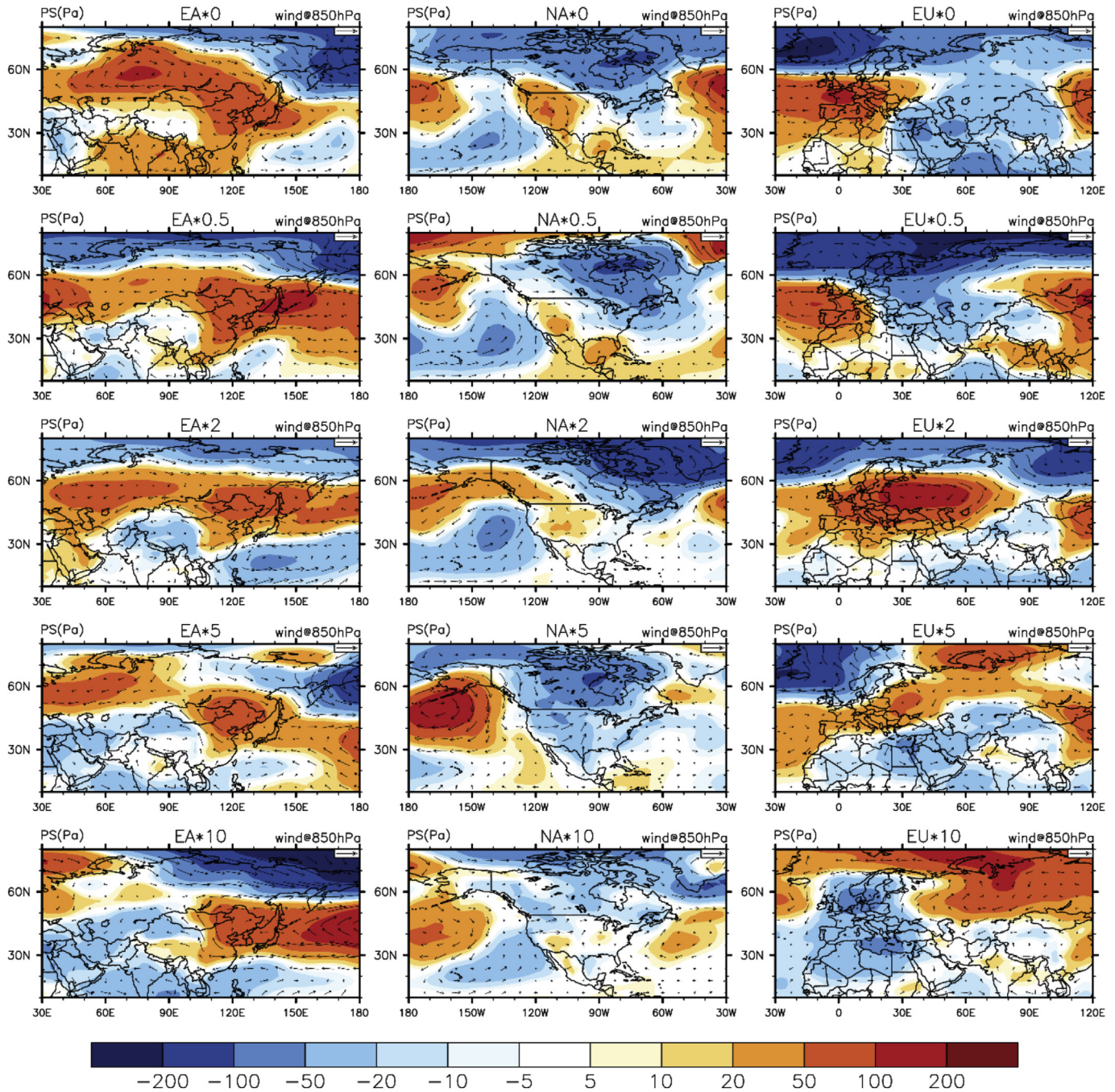


Fig. 11. Same as Fig. 6, but for surface pressure and wind field changes. The reference vector is 1 m/s.

Over Europe, a reduction of local BC emissions is associated with an intensified anti-cyclonic anomaly residing over eastern Atlantic and the entire EU between 30°N and 60°N. This pressure anomaly pattern facilitates the exchange of air mass between south and north, resulting in a warmer tendency over north EU and a cooling tendency over south AF. As EU BC emissions increase, an anti-cyclonic anomaly initially above EU tends to move northeastward, and is gradually replaced by a cyclonic anomaly, which warms the air mass over EU. This may explain the linear emissions-temperature relationship over the Mediterranean Sea and North Africa.

Above analysis indicates that though the change in BC emissions

influences atmospheric absorption of solar radiation, the atmospheric temperature change is largely determined by the BC induced circulation pattern and hydrological cycle changes (Ramanathan et al., 2001). Similarly, Chung et al. (2002) found that aerosol forcing in South Asia could weaken the north–south temperature gradient in the lower atmosphere, resulting in an enhancement of the area mean low-level convergence and a northward shift of the ITCZ. The consistent emission-temperature relationship is rarely observed and typically emerges outside of source region. In most cases, local temperature response towards emission changes follows a nonlinear relationship.

5. Conclusions

This study employs a fully-coupled earth system model CESM to evaluate the sensitivity of global short-term response of air quality and climate to the change of BC emissions from East Asia, North America and Europe. Specifically, for each region all anthropogenic BC emissions are multiplied by a scaling factor of 0, 0.5, 1, 2, 5, or 10. In each sensitivity run, a 10-year fully-coupled simulation is conducted and the results are compared to the base simulation (i.e., BC emissions are unchanged) to derive the corresponding estimates of BC emissions from a continental region resulting in or contributing to the perturbations of domestic and foreign air quality and climate. Rather than relying on a fixed sea surface temperature (SST), this study keeps ocean model active and focuses on the initial response. Therefore, the resulting changes in climate system are far from equilibrium, and should represent the initial climate evolution from a specific configuration of initial conditions. Though with some limitations, it may help to understand the possible outcomes of air quality and climate change if policies on BC mitigation in a specific region are either tightened or relaxed.

For all regions, a change in BC emissions will linearly influence BC concentrations over both source and nearby downwind regions even with the adjustment of regional climate perturbation. However, this linear source-receptor relationship does not persist in a hemispheric scale, especially between two regions with large BC sources (e.g., EA-NA, or NA-EU), mainly due to the climate induced concentration changes at the receptor region. This indicates for air quality purposes, controlling BC emissions will proportionally reduce local BC concentrations and improve domestic air quality. Its effect on long-range transport is complex when the effects of chemistry–climate interaction are taken into account.

The change in BC emissions not only influences ambient BC concentrations, but also affects the evolution of other chemical constituents, leading to an AOD perturbation beyond the source region. For most cases, a change in BC emissions in any of EA, NA or EU will induce a large AOD perturbation over the deserts in North Africa and Mongolia because dust entrainment and deposition are sensitive to BC induced climate changes (i.e., wind velocity and precipitation). Sometimes, the largest AOD change appears outside of the source region. This indicates that chemistry–climate interactions could be propagated to other regions via atmospheric circulation and might be intensified overseas when the intrinsic chemistry is sensitive to climate change.

Similar to the relationship between BC emissions and AOD changes, perturbations of radiative flux at TOA are generally in line with BC emission changes, with a linear relationship (i.e., $R^2 > 0.8$) spreading only above the source region. This indicates that a reduction (enhancement) of BC emissions leads to a radiative cooling (warming) effect on local atmosphere, except the places where cloud properties are strongly modified. However, even over the source region, this radiative forcing is not able to modify local temperature consistently. Higher degree of linearity ($R^2 > 0.8$) between 850 hPa temperature and BC emission changes appears only limited to a narrow belt close to the emission source. This is because the change of temperature is also significantly influenced by the perturbation of high/low pressure system as well as wind fields, which exchange warm/cool air mass meridionally. However, the magnitude and location of pressure and wind field anomalies vary irregularly with BC emission changes. This emphasizes the need to quantitatively understand the mechanism and major processes of the response of dynamical climate system to an anthropogenic forcer from regional to global scales.

Due to the complexity of chemistry–climate interactions (Isaksen et al., 2009; Raes et al., 2010) as well as uncertainty in emissions, transport, chemistry, and dry/wet depositions (Liu et al.,

2011; Shen et al., 2014), the climatic forcing of BC emissions unveiled in this work is subject to the preciseness of modeling individual physical, chemical and dynamical processes as well as how the model is configured, e.g., how the microphysics and chemical aging of BC are described, how the ocean component interacts with the atmosphere (fixed SST or active ocean) and how the direct, semi-direct and indirect of BC climatic forcing are treated. Uncertainty ranges associated to these processes are usually poorly quantified and examining the overall uncertainties is extremely challenging. In addition, the short-term climatic response of BC emissions is only statistically revealed, and the extent to which the effects are caused by the internal climate variability has not been fully addressed. These uncertainties will be partially resolved by advances in model development as well as conducting more sensitivity tests with different model configurations and in different climate model systems in the follow-up studies.

Acknowledgment

We thank Louisa Emmons, Xiaoyuan Li as well as two anonymous reviewers for their helpful suggestions on this study. This work was supported by funding from the National Natural Science Foundation of China under awards 41222011 and 41390240, the Research Project of the Chinese Ministry of Education No. 113001A, the “863” Hi-Tech R&D Program of China under Grant No. 2012AA063303, the 111 Project (B14001) as well as the undergraduate student research training program.

Appendix A. Supplementary data

Supplementary data related to this article can be found at <http://dx.doi.org/10.1016/j.atmosenv.2015.07.001>.

References

- Ban-Weiss, G.A., Cao, L., Bala, G., Caldeira, K., 2012. Dependence of climate forcing and response on the altitude of black carbon aerosols. *Clim. Dyn.* 38, 897–911.
- Bond, T.C., Streets, D.G., Yarber, K.F., Nelson, S.M., Woo, J.H., Klimont, Z., 2004. A technology-based global inventory of black and organic carbon emissions from combustion. *J. Geophys. Res. Atmos.* 109 (1984–2012).
- Bond, T.C., Doherty, S.J., Fahey, D., Forster, P., Bernsten, T., DeAngelo, B., Flanner, M., Ghan, S., Kärcher, B., Koch, D., 2013. Bounding the role of black carbon in the climate system: a scientific assessment. *J. Geophys. Res. Atmos.* 118, 5380–5552.
- Boville, B.A., Rasch, P.J., Hack, J.J., McCaa, J.R., 2006. Representation of clouds and precipitation processes in the community atmosphere model version 3 (CAM3). *J. Clim.* 19, 2184–2198.
- Cappa, C.D., Onasch, T.B., Massoli, P., Worsnop, D.R., Bates, T.S., Cross, E.S., Davidovits, P., Hakala, J., Hayden, K.L., Jobson, B.T., 2012. Radiative absorption enhancements due to the mixing state of atmospheric black carbon. *Science* 337, 1078–1081.
- Chung, C.E., Ramanathan, V., Kiehl, J.T., 2002. Effects of the South Asian absorbing haze on the northeast monsoon and surface-air heat exchange. *J. Clim.* 15, 2462–2476.
- Chung, S.H., Seinfeld, J.H., 2002. Global distribution and climate forcing of carbonaceous aerosols. *J. Geophys. Res. Atmos.* 107 (AAC 14–11-AAC), 14–33 (1984–2012).
- Chung, S.H., Seinfeld, J.H., 2005. Climate response of direct radiative forcing of anthropogenic black carbon. *J. Geophys. Res. Atmos.* 110 (1984–2012).
- Collins, W.D., Rasch, P.J., Boville, B.A., Hack, J.J., McCaa, J.R., Williamson, D.L., Kiehl, J.T., Briegleb, B., Bitz, C., Lin, S., 2004. Description of the NCAR Community Atmosphere Model (CAM 3.0). Tech. Rep. NCAR/TN-464+STR.
- Denman, K.L., Brasseur, G., Chidthaisong, A., Ciais, P., Cox, P.M., Dickinson, R.E., Hauglustaine, D., Heinze, C., Holland, E., Jacob, D., 2007. Couplings between changes in the climate system and biogeochemistry. *Clim. Change* 2007, 541–584.
- Flanner, M.G., Zender, C.S., Randerson, J.T., Rasch, P.J., 2007. Present day climate forcing and response from black carbon in snow. *J. Geophys. Res. Atmos.* 112 (1984–2012).
- Forster, P., Ramaswamy, V., Artaxo, P., Bernsten, T., Betts, R., Fahey, D.W., Haywood, J., Lean, J., Lowe, D.C., Myhre, G., Nganga, J., Prinn, R., Raga, G., Schulz, M., Van Dorland, R., 2007. Changes in atmospheric constituents and in radiative forcing. In: Solomon, S., Qin, D., Manning, M., Chen, Z., Marquis, M., Averyt, K.B., Tignor, M., Miller, H.L. (Eds.), *Climate Change 2007: The Physical*

- Science Basis. Contribution of Working Group I to the Fourth Assessment Report of the Intergovernmental Panel on Climate Change. Cambridge University Press, Cambridge, United Kingdom and New York, NY, USA.
- Hansen, J., Sato, M., Ruedy, R., 1997. Radiative forcing and climate response. *J. Geophys. Res. Atmos.* 102, 6831–6864 (1984–2012).
- Hansen, J., Sato, M., Ruedy, R., Nazarenko, L., Lacis, A., Schmidt, G., Russell, G., Aleinov, I., Bauer, M., Bauer, S., 2005. Efficacy of climate forcings. *J. Geophys. Res. Atmos.* 110 (1984–2012).
- Haywood, J., Shine, K., 1995. The effect of anthropogenic sulfate and soot aerosol on the clear sky planetary radiation budget. *Geophys. Res. Lett.* 22, 603–606.
- Heintzenberg, J., Charlson, R.J., 2009. *Clouds in the Perturbed Climate System: Their Relationship to Energy Balance, Atmospheric Dynamics, and Precipitation*. MIT Press, Cambridge, MA.
- Holtzlag, A., Boville, B., 1993. Local versus nonlocal boundary-layer diffusion in a global climate model. *J. Clim.* 6, 1825–1842.
- Isaksen, I., Granier, C., Myhre, G., Bernsten, T., Dalsøren, S., Gauss, M., Klimont, Z., Benestad, R., Bousquet, P., Collins, W., 2009. Atmospheric composition change: climate–chemistry interactions. *Atmos. Environ.* 43, 5138–5192.
- Jacobson, M.Z., 2010. Short-term effects of controlling fossil-fuel soot, biofuel soot and gases, and methane on climate, Arctic ice, and air pollution health. *J. Geophys. Res. Atmos.* 115 (1984–2012).
- Lamarque, J., Emmons, L., Hess, P., Kinnison, D.E., Tilmes, S., Vitt, F., Heald, C., Holland, E.A., Lauritzen, P., Neu, J., 2012. CAM-chem: description and evaluation of interactive atmospheric chemistry in the community earth system model. *Geosci. Model Dev.* 5, 369–411.
- Liu, J., et al., 2009. Evaluating inter-continental transport of fine aerosols: (1) Methodology, global aerosol distribution and optical depth. *Atmos. Environ.* <http://dx.doi.org/10.1016/j.atmosenv.2009.03.054>.
- Liu, J., Fan, S., Horowitz, L.W., Levy, H., 2011. Evaluation of factors controlling long-range transport of black carbon to the Arctic. *J. Geophys. Res. Atmos.* 116 (1984–2012).
- Liu, Y., Liu, J., Tao, S., 2013. Interannual variability of summertime aerosol optical depth over East Asia during 2000–2011: a potential influence from El Niño Southern Oscillation. *Environ. Res. Lett.* 8, 044034.
- Menon, S., Hansen, J., Nazarenko, L., Luo, Y., 2002. Climate effects of black carbon aerosols in China and India. *Science* 297, 2250–2253.
- Neale, R.B., Chen, C.-C., Gettelman, A., Lauritzen, P.H., Park, S., Williamson, D.L., Conley, A.J., Garcia, R., Kinnison, D., Lamarque, J.-F., 2010. Description of the NCAR Community Atmosphere Model (CAM 5.0). NCAR Tech. Note NCAR/TN-486+STR.
- Onischuk, A., Di Stasio, S., Karasev, V., Baklanov, A., Makhov, G., Vlasenko, A., Sadykova, A., Shipovalov, A., Panfilov, V., 2003. Evolution of structure and charge of soot aggregates during and after formation in a propane/air diffusion flame. *J. Aerosol Sci.* 34, 383–403.
- Oshima, N., Koike, M., Zhang, Y., Kondo, Y., Moteki, N., Takegawa, N., Miyazaki, Y., 2009. Aging of black carbon in outflow from anthropogenic sources using a mixing state resolved model: model development and evaluation. *J. Geophys. Res. Atmos.* 114 (1984–2012).
- Raes, F., Liao, H., Chen, W.T., Seinfeld, J.H., 2010. Atmospheric chemistry–climate feedbacks. *J. Geophys. Res. Atmos.* 115 (1984–2012).
- Ramanathan, V., Crutzen, P., Kiehl, J., Rosenfeld, D., 2001. Aerosols, climate, and the hydrological cycle. *science* 294, 2119–2124.
- Ramanathan, V., Chung, C., Kim, D., Bettge, T., Buja, L., Kiehl, J., Washington, W., Fu, Q., Sikka, D., Wild, M., 2005. Atmospheric brown clouds: impacts on South Asian climate and hydrological cycle. *Proc. Natl. Acad. Sci. U. S. A.* 102, 5326–5333.
- Samsel, B., Myhre, G., Schulz, M., Balkanski, Y., Bauer, S., Bernsten, T., Bian, H., Bellouin, N., Diehl, T., Easter, R.C., 2013. Black carbon vertical profiles strongly affect its radiative forcing uncertainty. *Atmos. Chem. Phys.* 13, 2423–2434.
- Sand, M., Bernsten, T., Kay, J., Lamarque, J., Seland, Ø., Kirkevåg, A., 2013. The Arctic response to remote and local forcing of black carbon. *Atmos. Chem. Phys.* 13, 211–224.
- Shen, Z., Liu, J., Horowitz, L., Henze, D., Fan, S., Mauzerall, D., Lin, J.-T., Tao, S., 2014. Analysis of transpacific transport of black carbon during HIPPO-3: implications for black carbon aging. *Atmos. Chem. Phys.* 14, 6315–6327.
- Shindell, D., Faluvegi, G., 2009. Climate response to regional radiative forcing during the twentieth century. *Nat. Geosci.* 2, 294–300.
- Shine, K.P., Cook, J., Highwood, E.J., Joshi, M.M., 2003. An alternative to radiative forcing for estimating the relative importance of climate change mechanisms. *Geophys. Res. Lett.* 30.
- Sokolov, A.P., 2006. Does model sensitivity to changes in CO₂ provide a measure of sensitivity to other forcings? *J. Clim.* 19, 3294–3306.
- Tie, X., Brasseur, G., Emmons, L., Horowitz, L., Kinnison, D., 2001. Effects of aerosols on tropospheric oxidants: a global model study. *J. Geophys. Res. Atmos.* 106, 22931–22964 (1984–2012).
- Wesely, M., 1989. Parameterization of surface resistances to gaseous dry deposition in regional-scale numerical models. *Atmos. Environ.* 23, 1293–1304 (1967).
- Zhang, G.J., McFarlane, N.A., 1995. Role of convective scale momentum transport in climate simulation. *J. Geophys. Res. Atmos.* 100, 1417–1426 (1984–2012).
- Zhang, Y., Sun, S., Olsen, S.C., Dubey, M.K., He, J., 2011. CCSM3 simulated regional effects of anthropogenic aerosols for two contrasting scenarios: rising Asian emissions and global reduction of aerosols. *Int. J. Climatol.* 31, 95–114.